Research paper

First order risk assessment for nanoparticle inhalation exposure during injection molding of polypropylene composites and production of tungsten-carbide-cobalt fine powder based upon pulmonary inflammation and surface area dose

Antti Joonas Koivisto [a,*], Kirsten Inga Kling [a], Marcus Levin [a], Wouter Fransman [b], Ilse Gosens [c], Flemming Ralph Cassee [c,d], Keld Alstrup Jensen [a]

[a] National Research Centre for the Working Environment, Lersø Parkallé 105, Copenhagen DK-2100, Denmark
[b] TNO, PO Box 360, 3700AJ Zeist, The Netherlands
[c] National Institute for Public Health and the Environment (RIVM), Bilthoven, The Netherlands
[d] Environmental Epidemiology, Institute of Risk Assessment Sciences, Utrecht University, TD Utrecht, The Netherlands

ARTICLE INFO

ABSTRACT

Inhalation exposure to low toxicity and biodurable particles has shown to induce polymorphonuclear neutrophilia (PMN) in the lungs, which is a strong indicator for lung inflammation. Recently, Schmid and Stoeger (2016; http://dx.doi.org/10.1016/j.jaerosci.2015.12.006) reviewed mice and rat intratracheal instillation studies and assessed the relation between particles dry powder BET surface area dose and PMN influx for granular biodurable particles (GBPs) and transition metal oxides. In this study, we measured workers alveolar lung deposited surface area (LDSA) concentrations ($\mu m^2 \, cm^{-3}$) during injection molding of polypropylene (PP) car bumpers and production of tungsten-carbide-cobalt (WCCo) fine grade powder using diffusion chargers. First order risk assessment was performed by comparing the doses calculated from measured LDSA concentrations during an 8-h work day with the $NOEL_{1/100}$, the one hundredth of no observed effect level, assigned for GBPs ($0.11 \, cm^2 \, g^{-1}$) and transition metal oxide particles ($9 \times 10^{-3} \, cm^2 \, g^{-1}$). During the injection molding of PP car bumpers, LDSA concentrations varied from 23 to 39.8 $\mu m^2 \, cm^{-3}$. During 8-h exposure PP, particle doses were at a maximum of $1.4 \times 10^{-3} \, cm^2 \, g^{-1}$, which was a factor 100 lower compared to the $NOEL_{1/100}$ assigned for GBPs. In the WCCo fine powder production plant, the LDSA concentrations were below 18.7 $\mu m^2 \, cm^{-3}$, which corresponds to the 8-h dose of $2.7 \times 10^{-3} \, cm^2 \, g^{-1}$. This is 3 times lower than the $NOEL_{1/100}$ assigned for transition metal oxide particles. The LDSA concentrations were generally low compared to urban background levels of 44.2 $\mu m^2 \, cm^{-3}$ in European cities.

1. Introduction

In an occupational environment, particle concentrations in air can be highly elevated compared to the background due to high energy processes and use of chemicals that lead to particle formation (Hämeri et al., 2009). Process generated particles and increasing use of engineered nanomaterials (Vance et al., 2015) present new challenges to understand exposure, hazard and risk management in occupational environments (Hämeri et al., 2009; Pietroiusti and Magrini, 2014; Bekker et al., 2015).

Currently, only few occupational exposure limit values exist for particulate matter (PM) and are usually given in inhalable (PM_{10}; $D_p \leq 10 \, \mu m$) or respirable ($PM_{4.0}$; $D_p \leq 4.0 \, \mu m$) mass concentration (Cherrie et al., 2013; Kuempel et al., 2014). However, many studies have shown that PM_{10} or $PM_{4.0}$ mass concentration is only a rough indicator for a biologically effective dose of the complex mixture of airborne particles (Oberdörster, 2000; Maynard and Kuempel, 2005; Borm et al., 2007; Wittmaack, 2007; Gebel, 2012; Simkó et al., 2014; Schmid and Stoeger, 2016; Braakhuis et al., 2016). There is a need to develop risk assessment techniques where PM exposure and dose assessment is closely related to the biological response (Pietroiusti and Magrini, 2014).

For regulatory purposes and efficient hazard assessment, nanomaterials can be grouped according to their intrinsic physical properties and biological interactions (Arts et al., 2014, 2015, 2016; Braakhuis et al., 2016; Dekkers et al., 2016; Godwin et al., 2015). Granular biodurable particles (GBPs) are the largest material group considering their material production volumes and use (Piccinno et al., 2012). GBPs are classified as low toxicity particles (Moreno-Horn and Gebel, 2014; Arts et al., 2016) although all GBPs may cause inflammation depending on the deposited dose. Ongoing inflammatory processes may cause secondary mutagenicity that may finally lead to lung cancer

* Corresponding author.
  E-mail address: jok@nrcwe.dk (A.J. Koivisto).

(Gebel et al., 2014). The total particle surface area (cm^2) that is deposited in the lung (lung deposited surface area; LDSA) is recognized to be a relevant dose metric to describe toxicological outcomes for a range of different sizes of GBPs of the same chemical composition and morphology after inhalation (Oberdörster et al., 2005; Stoeger et al., 2007, 2009; Waters et al., 2009; Braakhuis et al., 2016; Schmid and Stoeger, 2016).

An influx of polymorphonuclear neutrophils (PMNs) in the lungs is a hallmark of the onset of inflammation after PM exposure (Grommes and Soehnlein, 2011). Lung inflammation is expected to be associated with the dose in the alveolar region of the respiratory tract (Nieboer et al., 2005) which is why LDSA is expected to more accurately define the dose-response relationship (Lison et al., 2014). For example, for TiO$_2$ particles of two different sizes with the instilled dose expressed as mass, nano-sized particles induce a greater inflammatory response in the lung than micron-sized particles. However, with the dose expressed as particle surface area, the neutrophil responses fitted the same dose-response curve (Oberdörster et al., 2005).

In this study, we measured workers exposures in a factory producing polypropylene (PP) car bumpers with injection molding and in a tungsten-carbide-cobalt (WCCo) fine grade powder production plant. The PP was colored using organic pigment nanoparticles and WCCo is classified as nanomaterial. In both facilities the exposure to engineered nanomaterials cannot be ruled out, therefore a Tier 2 exposure assessment was performed (OECD, 2015). PM concentrations were measured from near field (NF) and far field (FF) with two miniature diffusion size classifiers and airborne particles were collected for Transmission Electron Microscopy (TEM) analysis. A first order risk assessment for inhalation exposure based on pulmonary inflammation was performed by assuming that the PMN surface area dose-responses assigned by Schmid and Stoeger (2016) can be compared to the doses calculated from measured LDSA concentrations during 8-h exposure.

2. Materials and methods

2.1. Injection molding

An injection molding machine (Engel, 2500 tons, Engel Austria GmbH, A-4311 Schwertberg) was used to manufacture PP components with a weight of 1.59 kg. Three different PP materials were molded:

- Natural color PP (PP$_0$; KSR4525, Borealis AG, Vienna, Austria)
- PP containing 20 wt% mineral filler (PP$_H$; Hifax TRC 221P/2 G14008 OTOPHT, Mat no.: 19301A42, LyondellBasell, Ferrata, Italy)
- PP containing 0.2 wt% organic pigment (PP$_{OP}$; di-keto-pyrrolo-pyrrole pigment, CAS-Nr. 84632-65-5, SUN FP-7 project provided by BASF Schweiz AG, Switzerland; see also Sotiriou et al., 2016)

Injection molding was performed in a naturally ventilated industrial hall (area > 2500 m^2; T = N/A; RH = N/A; Fig. 1a). In addition to the injection molding, an electric forklift was used occasionally. During the second, day painting was performed in a paint booth approximately 30 m from the injection molding area. A blow torch was used occasionally to smooth PP bumper holder parts which were cut off with a knife.

2.2. Sieving and milling

WCCo fine powder was manufactured by fragmenting *ca.* 1 cm^3 WCCo pieces with a high energy ball mill (technical information N/A). The high energy ball mill was located in a ventilated cabin (air exchange ratio N/A) where the replacement air was unfiltered outdoor air from the production hall (Fig. 1b). After milling, the WCCo powder was sieved using a vibrating sieve with a 38 μm pore size. The material was added to the sieve *via* an open feed funnel which had local exhaust ventilation (volume flow N/A). The sieve was switched off when the bucket with sieved powder was replaced with an empty one. The sieve was located in a partly closed room located in the production hall (Fig. 1b). During the measurements, Iron-based, Nickel-based and Titanium-based powders were milled and handled in other parts of the facility. During the work tasks, workers wore filtering facepiece respirators (type FFP2, manufacturer N/A).

2.3. Measurement strategy

Particle concentrations were measured with two Miniature Diffusion Size Classifiers with a 0.7 μm pre-separator (DiSCmini, Matter Aerosol AG, Wohlen, Switzerland). During the injection molding, concentrations were measured simultaneously 1.5 m from the mold and from a workstation (Fig. 1a). In the WCCo fine powder production, concentrations were measured simultaneously 0.5 m from the sieve and from in the process hall or the high energy mill cabinet and the process hall (Fig. 1b).

The DiSCmini instrument functions through unipolar charging of particles and detection of their carried charge in two electrometer stages. In the first stage, the diffusion stage, where particles are detected mainly due to their inherent Brownian motion. In the second stage, the filter stage, the remainder of the particles is detected. Based on the ratio of the two electrometer signals, an average particle size, D_p, can be calculated as smaller particles undergo larger Brownian motion and will thus be more likely to be detected in the first stage (Fierz et al., 2011). This average particle size can then be used to calculate a number concentration, assuming a Geometric Standard Deviation (GSD) of 1.7,
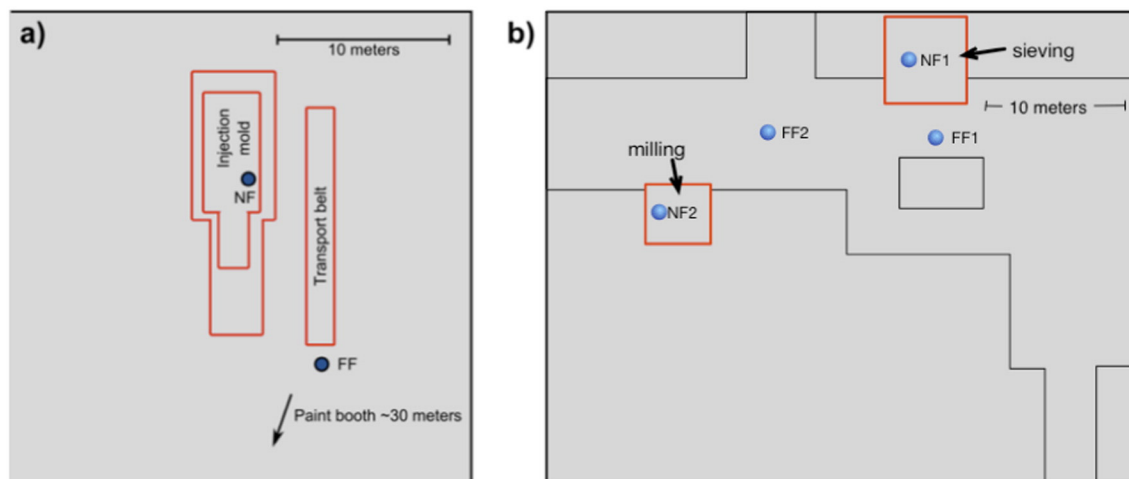

Fig. 1. Layout of the process areas a) in the injection molding and b) in the WCCo sieving and milling.

from the summed measured currents as the efficiency of the charging is known to be proportional to $D_p^{1.1}$. It has been shown that the DiSCmini measures particle number concentration within ± 30% as compared to results from Condensation Particle Counters (CPC) and Scanning Mobility Particle Sizers (SMPS; Fierz et al., 2011, Asbach et al., 2012). However, Bau et al. (2014) reported cases of poorer correlation, with ratios ranging from − 51% to + 65% as compared to a CPC. They also reported the Geometric Mean Diameter (GMD) to be within ± 38% as compared to a SMPS. Furthermore, Fierz et al. (2011) showed that the particle size measured by the DiSCmini was underestimated for narrow size distributions (GSD < 1.5) and overestimated for wide distributions (GSD > 2.1).

For particles smaller than 300 nm there is a good correlation between the total current carried by the aerosol particles and the alveolar LDSA (Asbach et al., 2009). Fierz et al. (2011) reported a ± 20% measurement ratio in the size range of 16 to 240 nm. Todea et al. (2015) reported that alveolar LDSA measurements were within ± 30% of theoretical values for particles between 20 and 400 nm. Furthermore they reported that the DiSCmini underestimates the alveolar LDSA for 20 nm particles and for large size particles (− 62% for 685 nm particles).

2.4. Particle characterization

Airborne particles were collected on Cu TEM grids with formvar carbon foil (Plano, Wetzlar, Germany) using a mini particle sampler ($Q_s =$ 0.58 L min^{-1}; Ecomeasure, Saclay, France; R'mili et al., 2013). Samples were analyzed in a TEM Tecnai T20 G2 (FEI, Eindhoven, The Netherlands) operated at 200 kV. High-resolution (9.1625 pixel/nm) to overview (0.0045 pixel/nm) images were recorded with DigitalMicrograph software (Gatan Inc., Pleasanton, VA, USA) using a bottom mounted camera (Gatan US1000). For size analysis, overview images were post processed with ImageJ 1.50i software (W. Rasband, National Institute of Health, USA). The diameter discussed in connection with the microscopy images refers to equivalent area diameter of a circle of the pixel size.

2.5. Estimation of the risk to develop pulmonary inflammation

Recently, Schmid and Stoeger (2016) studied the acute influx of PMNs into the lungs of rats and mice after single intratracheal instillation exposure to spherical particles, expressed as function of dose per BET surface area normalized with lung weight. The studied materials comprised polystyrene, two types of titanium dioxides, six types of carbonaceous materials, hydrothermally synthesized α-crystalline silica, and Co-, Ni-, and Zn transition metal oxides. The relation of dry powder BET surface area dose normalized with the lung weight $D_{SA,BET}$ (cm^2 g^{-1}) and PMNs (%) expressed as number of PMN cells normalized to total number of cells was

$$PMN\,(\%) = 11.0 \times \ln(D_{SA,BET}) - 26.7.$$

The maximum observed PMN level accounted for 60% of the total number of cells; the geometric mean of half the maximal effective dose for PMNs was 175 cm^2 g^{-1} (GSD 2.2) for GBPs and 15 cm^2 g^{-1} for transition metal oxide particles. The PMN no observed effect level (NOEL; no inflammation) was between 0 and 5% corresponding to a GBP dose between 11 and 18 cm^2 g^{-1}. The NOEL level was divided with a default 100-fold factor (NOEL$_{1/100}$) to take inter-species variation between mice or rats and intra-species variation between humans into account (ECHA, 2009). This corresponds to a NOEL$_{1/100}$ of 0.11 cm^2 g^{-1} for GBPs and 9×10^{-3} cm^2 g^{-1} for transition metal oxides.

The surface area dose (cm^2) was calculated by multiplying the LDSA concentration (μm^2 cm^{-3}), measured with a DiSCmini, by a certain volume of inhaled air (12 m^3: the inhalation rate for a 70 kg male during light exercise is 25 L min^{-1} (Freijer et al., 1997; ECHA, 2016) which corresponds to a total inhaled volume of 12 m^3 during 8-h breathing). The

surface area dose was normalized using the weight of the lungs from a normal male of 840 g (Molina and DiMaio, 2012). The human equivalent surface area dose (cm^2 g^{-1}) was compared with the NOEL level to estimate a workers risk for acute lung inflammation by following the conceptual approach presented by Oller and Oberdörster (2010). The risk assessment is performed with the following critical assumptions:

1) *Particles emitted by the processes are spherical and comparable in inflammatory responses to GBPs and transition metal oxide particles used in Schmid and Stoeger (2016).* The particles in the injection molding were somewhat spherical (Fig. 5), and PP is a hydrophobic and inert material that does not degrade *in vivo* (Maintz, 2015). In the WCCo production plant, particles containing W, Ni, and Co were aggregated or agglomerated and their aspect ratio increased with increasing agglomerate/aggregate diameter (Fig. 6).

2) *The human equivalent deposited surface area dose is equal to the LDSA concentration × inhaled volume/lung weight.* LDSA concentration can be measured in an optimal case with an accuracy of ± 30% for particle sizes between 20 and 400 nm (Todea et al., 2015). The volume of inhaled air during 8-h may vary from *ca.* 5 m^3 to 50 m^3 if the work load varies from resting (*e.g.* monitoring) to heavy exercise (*e.g.* lifting; Freijer et al., 1997). The influence on the breathing volume by the human total body weight is relatively small; a 90 kg male would breathe 18% more air during 8-h than a 70 kg male (Freijer et al., 1997). Particle deposition efficiency depends on the inhalation rate (Hussain et al., 2011) and hygroscopic properties. Hydrophilic particles >100 nm in diameter may grow up to 4 times larger in 95% relative humidity (Vu et al., 2015). Healthy men aged 18 to 35 years with a total body weight between 48.5 and 153 kg have a mean weight of the right lung of 445 g (range from 185 to 967 g) and the left lung of 395 g (range from 186 to 885 g) while lung weights in women are *ca.* 25% smaller (Molina and DiMaio, 2012).

3) *The dry powder BET surface area corresponds to the LDSA.* Particle surface area depends on the measurement technique (Ku and Maynard, 2005; Ku and Kulkarni, 2012). LeBouf et al. (2011) showed that the surface area measured with a diffusion charger differed from the filter-based inert gas adsorption (BET method) measurement technique 1.27 to 5.77 times for ultrafine particles and 0.39 to 0.75 times for fine particles for TiO$_2$ particles at low and high concentration, respectively.

4) *An equal instilled dose is equivalent to the inhaled alveolar dose calculated from LDSA concentrations.* This is valid only if the particle deposition distribution to the lungs and lung clearances are similar after inhalation and instillation (Brown et al., 2005; Jarabek et al., 2005). A high dose rate following intratracheal instillation may overwhelm alveolar macrophages which may lead to dysfunction and reduction of lung clearance and alter the toxicological response (Baisch et al., 2014; Morimoto et al., 2016). To our knowledge, the fraction of material reaching the alveoli after instillation has not yet been studied. Therefore, we make the above assumption.

5) *An equal PMN response is assumed to occur at an equivalent dose in both rats and mice (based on intratracheal instillation studies) and humans (based on inhalation exposure).* Here, the dose was normalized with the lung weight, even though alveolar surface area is often considered as an appropriate dose metric to correlate with pulmonary inflammation (Jarabek et al., 2005; Oller and Oberdörster, 2010). Intratracheal instillation studies have shown to cause equal or greater inflammation compared to the inhalation of nanoparticles (Baisch et al., 2014; Morimoto et al., 2016; Horie et al., 2016). A 10-fold factor was assigned for inter-species variation and a 10-fold factor for differences between species (ECHA, 2009). Shape and slope of the dose-response for transition metal oxide particles was assumed to be the same as for GBPs. However, the potency is larger as a PMN increase occurring at 12 times smaller concentrations compared to GBPs (Schmid and Stoeger, 2016).

Table 1
Uncertainties and knowledge gaps in exposure-, dose-, and dose-response assessment.

Exposure assessment		Dose assessment		Dose-response assessment	
Quantity or assumption	Uncertainty	Quantity or assumption	Uncertainty	Quantity or assumption	Uncertainty
Exposure level	˃ ± 30%	Inhaled volume during 8-h	N/A; 10-fold if there is no information about work load	Dry powder BET surface area ≡ LDSA	>10-fold
Morphology and composition of particle concentrations	Qualitative information only	Human weight influence on inhaled volume for 70 and 90 kg persons	ca. ± 20%	Instilled dose ≡ calculated inhaled alveolar dose	Dose distribution N/A; biological half time N/A but expected to be higher in instillation than in inhalation exposure
Injection molding: PP ≡ GBPs	N/A	Change in particle deposition efficiency due to breathing and change in particle size	ca. ± 20%	Dose response in instilled dose ≡ inhaled dose	N/A but higher dose response is expected in instilled dose than inhaled dose
WCCo production particles ≡ transition metal oxides	N/A	Weight of lungs	Range from 371 to 1852 g in men (44 to 220%) Lungs in women are on average 25% smaller than in men.	Inter-species variation factor intra-species variation factor 95% limits for GBPs NOEL level of 11 cm^2 g^{-1} Transition metal oxide particles PNM response is 12 times smaller than GBPs response.	10-fold 10-fold 2.3 to 53 cm^2 g^{-1} N/A

The uncertainties or extrapolation factors are usually not known or in range of an order of magnitude (Table 1).

3. Results

3.1. Injection molding

During injection molding of car bumpers, the particle number and $LDSA$ concentrations in the near field (N_{NF} and $LDSA_{NF}$) remained at similar levels as FF concentrations (Table 2, Figs. 2 and 3). Opening of the mold and removal of the bumper did not elevate the concentrations notably (Figs. 2 and 3). The PP filler did not effect on the emissions notably. The geometric mean $LDSA_{NF}$ levels were at their maximum 10% higher than respective $LDSA_{FF}$ concentrations, which was mainly caused by residual particles from the polishing process at day 2 (ending at ca. 00:50, see Fig. 3b). Thus, the particle concentrations from injection molding of car bumpers were too low to detect with the DiSCmini's.

The PP material change showed increased ≤10% N_{NF} and ≤33% $LDSA_{NF}$ geometric mean concentrations compared to the respective FF concentrations. This was mainly caused by an increase in NF particle sizes that were 6 to 23% larger in diameter, compared to the FF particles (Table 2). Particle size increase was significant especially during day 1 between 03:25 and 04:15 (Fig. 2c). This indicates that particles released from injection mold polishing process are larger than particles released during the injection molding process. This explains why the particle number concentration, which is proportional to D_p^0, remained at similar level, but the LDSA concentration, which is proportional to ca. D_p^1, were increased. The particle emissions during change of one PP material to another increased both the NF and FF concentrations (Figs. 2 and 3). The particles analyzed on the TEM grids show patterns that suggest that large droplets were collected and material recrystallized on the substrate (Fig. 5a and b). The average diameter of these (presumably recrystallized) particles is 56.8 nm (standard deviation 34.9; min 10.1; max 126.6 nm) and their aspect ratio is 1.44 (standard deviation 0.29). In the size range below 50 nm, particles are mainly composed of C, whereas in larger particles, S, Na and K are found (Fig. 5).

3.2. WCCo sieving and milling

Both in sieving and milling, the N_{NF} and $LDSA_{NF}$ concentrations were 16 to 29% lower as in the FF (Table 2, Fig. 4) during the same processes. The NF particle sizes were similar in the sieving process, but 16% lower in the milling process as in the FF (Table 2). This suggests that the concentrations were similar in the production hall as at the process sites where the LDSA concentrations varied from 10 to 18.7 $μm^2$ cm^3.

Particle analysis on the TEM grids showed that the majority of WCCo particles were agglomerated, occurring in the size range of 274 nm to 10.6 μm as pure particles (Fig. 6). Some were observed as internally mixed in large, micrometer-sized aggregates with Ni-based particles (Fig. 6a). Large aggregates of Ni-based particles coated with C were observed in low number. The average aspect ratio of all analyzed particles is 1.48 (standard deviation 0.4).

3.3. Estimation of the workers risk for acute pulmonary inflammation

During the injection molding, the geometric mean $LDSA_{NF}$ concentrations were elevated and ranging 0.5 to 5.7 $μm^2$ cm^{-3}; during PP material change the $LDSA_{FF}$ concentration reached 10.0 $μm^2$ cm^3. This corresponds to 8-h doses of 0.07×10^{-3} to 0.8×10^{-3} cm^2 g^{-1} during the injection molding and 1.4×10^{-3} cm^2 g^{-1} during PP material change. Assuming that PP particles have similar properties than GBPs (Fig. 5), the doses are >80 times below the respective $NOEL_{1/100}$ level of 0.11 cm^2 g^{-1}.

Table 2
Geometric mean and standard deviation in brackets of particle number concentration, lung deposited surface area, and particle size in the near field and far field and their ratios as percentages.

Process	Near Field (NF)			Far Field (FF)			NF/FF–ratios × 100		
	$N_{NF} \times 10^3$ [cm^{-3}]	$LDSA_{NF}$ [$μm^2$ cm^{-3}]	$D_{p,NF}$ [nm]	$N_{FF} \times 10^3$ [cm^{-3}]	$LDSA_{FF}$ [$μm^2$ cm^{-3}]	$D_{p,FF}$ [nm]	N_{NF}/N_{FF} [%]	$LDSA_{NF}/LDSA_{FF}$ [%]	$D_{p,NF}/D_{p,FF}$ [%]
PP_H	9.8 (1.34)	25.2 (1.13)	46.9 (1.2)	9.6 (1.2)	23.0 (1.08)	44.3 (1.13)	101	110	106
Polishing PP_O	12.6 (1.35)	40.4 (1.62)	57.6 (1.36)	11.5 (1.13)	30.4 (1.31)	48.7 (1.21)	110	133	118
PP_0	7.2 (1.08)	28.6 (1.06)	70.6 (1.03)	8.9 (1.11)	28.1 (1.1)	57.6 (1.03)	81	102	123
PP_OP	14.8 (1.28)	45.5 (1.24)	55.5 (1.04)	15.5 (1.14)	39.8 (1.11)	47.6 (1.04)	96	114	117
Polishing PP_OP	14.6 (1.46)	49.6 (1.42)	60.9 (1.06)	13.5 (1.22)	39.6 (1.19)	53.8 (1.05)	108	125	113
Sieving	3.5 (1.16)	10.0 (1.07)	51.2 (1.1)	4.4 (1.2)	12.1 (1.09)	51.0 (1.17)	81	83	100
Milling	3.9 (1.23)	13.2 (1.27)	60.5 (1.17)	4.7 (1.26)	18.7 (1.32)	71.6 (1.15)	84	71	84
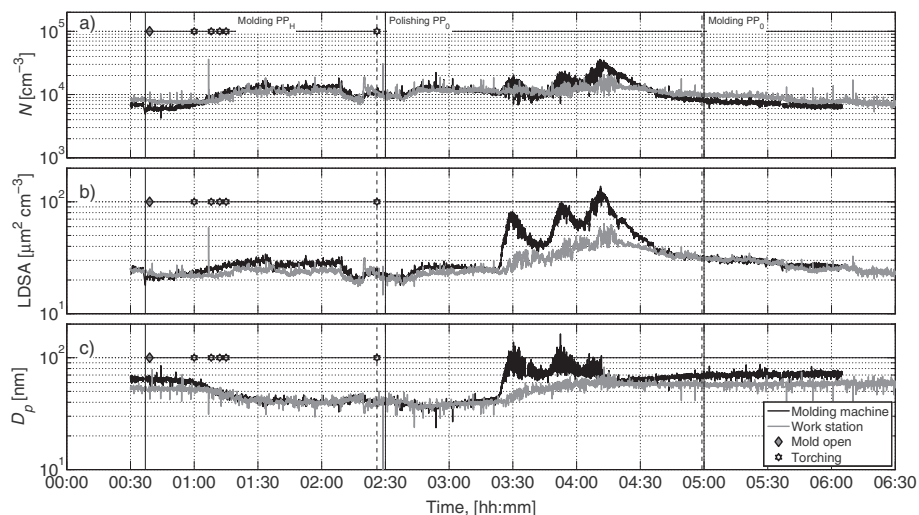
Fig. 2. Day 1 particle a) number and b) LDSA concentrations and c) average particle diameter during molding of PP_H, polishing the injection mold screw, process adjustment, and molding PP_0. Solid and dashed vertical lines show start and end of the process, respectively.

In the WCCo fine powder production plant, the 8-h dose was 2.7×10^{-3} cm^2 g^{-1} and the particles contained *e.g.* Ni, W, and Co transition metals (Fig. 6). Assuming that the dose consists of only transition metal oxides, the dose is *ca.* 3 times lower than the $NOEL_{1/100}$ level of 9×10^{-3} cm^2 g^{-1} for transition metal oxides.

4. Discussion

In the present study we used the LDSA exposure measurements from two work places to assess the risk for workers, to develop a pulmonary inflammation during 8-h exposures. The risk was estimated by comparing the dose levels calculated from LDSA exposure levels with the $NOEL_{1/100}$ levels derived from Schmid and Stoeger (2016). In injection molding at the worst case exposure scenario the dose was 80 times below the $NOEL_{1/100}$ level for GBPs and in the WCCo fine powder production plant 3 times below the $NOEL_{1/100}$ level for transition metal oxide particles.

It is expected that the injection molding process is safe to perform considering workers risk to suffer pulmonary inflammation for a single exposure day. In the WCCo fine powder production plant, it is suggested to perform more detailed exposure analysis to verify the actual dose level of transition metal oxide particles (*e.g.* assess fraction of transition metal oxides in the airborne PM or collect powder samples to assess

airborne BET surface area concentration) or reduce exposure levels using more effective local exposure controls. In the current exposure assessment, the use of personal protective equipment was not taken into account. According to Janssen et al. (2007) the protection factor of a properly used facepiece respirator is 119 (GSD 3.0). This should be enough to reduce the exposure at the level where pulmonary inflammation is not expected to occur.

Systematic measurements of the alveolar LDSA concentrations are still scarce but some first studies provide an overview of the exposure levels at urban environments, specific indoor environments, and occupational settings. The average urban alveolar LDSA concentrations vary in different cities from a geometric mean of 44.2 μm^2 cm^{-3} (GSD 2.2) in background measurement sites to geometric mean of 64.5 μm^2 cm^{-3} (GSD 1.9) in traffic areas (Ntziachristos et al., 2007; Buonanno et al., 2012; Gomes et al., 2012; Reche et al., 2011). Similar alveolar LDSA concentrations, ranging from *ca.* 20 to 60 μm^2 cm^{-3}, were measured in urban areas in Switzerland (Eeftens et al., 2015). The personal LDSA exposures in different urban microenvironments in Como, Italy, varied from *ca.* 10 to 90 μm^2 cm^{-3} (Spinazzè et al., 2015).

Occupational alveolar LDSA concentrations has been shown to be 360 μm^2 cm^{-3} in wood-fired ovens pizzerias in Italy (Buonanno et al., 2010) and in automotive plants 700 μm^2 cm^{-3} (arithmetic standard
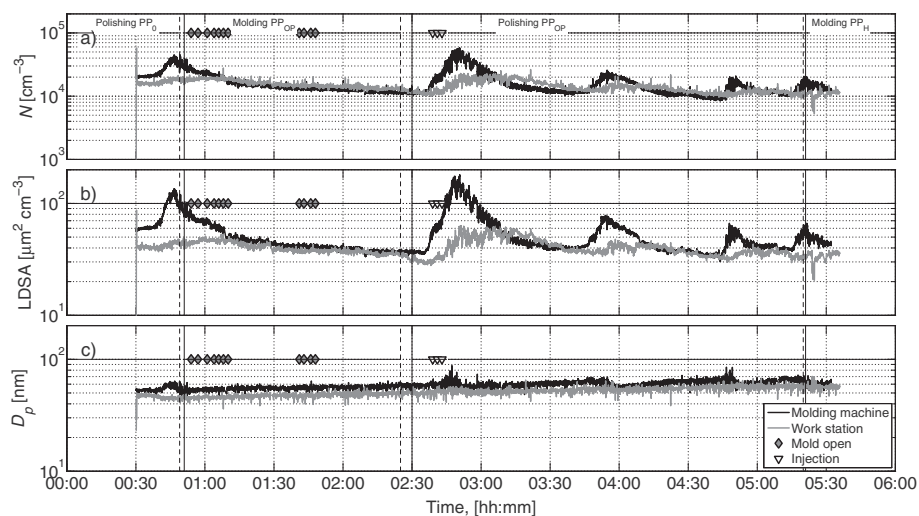
Fig. 3. Day 2 particle a) number and b) LDSA concentrations and c) average particle diameter during polishing the injection mold screw, molding PP_{OP}, polishing and cleaning the injection mold screw, and molding PP_H. Solid and dashed vertical lines show start and end of the process, respectively.
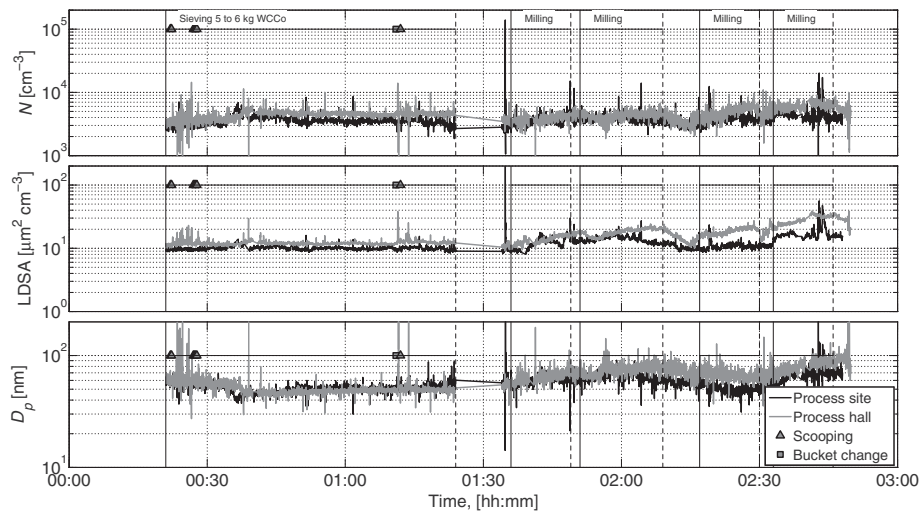
Fig. 4. Particle a) number and b) LDSA concentrations and c) average particle diameter during WCCo sieving and milling processes. Solid and dashed vertical lines show start and end of the process, respectively.

deviation 340 μm² cm⁻³; Buonanno et al., 2011). Geiss et al. (2016) measured average alveolar LDSA concentrations of 415 μm² cm⁻³ in a canteen kitchen, 77.2 μm² cm⁻³ in a car, and 137 μm² cm⁻³ during welding. In a private house with wood burning stove and gas cooking the average alveolar LDSA concentration was 54 μm² cm⁻³ (Geiss et al., 2016).

During the injection molding process, the NF and FF LDSA concentrations varied from 23.0 to 45.5 μm² cm⁻³ and the concentrations in the

NF were not elevated notably from the FF concentrations (Table 2). Similar results were measured by Boonruksa et al. (2016) during injection molding performed in an industrial laboratory. During the PP material change, the NF and FF LDSA concentrations in this study varied from 30.4 to 49.6 μm² cm⁻³ (Table 2). These concentrations are similar to urban background concentrations (Reche et al., 2011).

In the WCCo production plant, the DiSCmini signal was noisier in the WCCo sieving and milling than in the injection molding. This points to
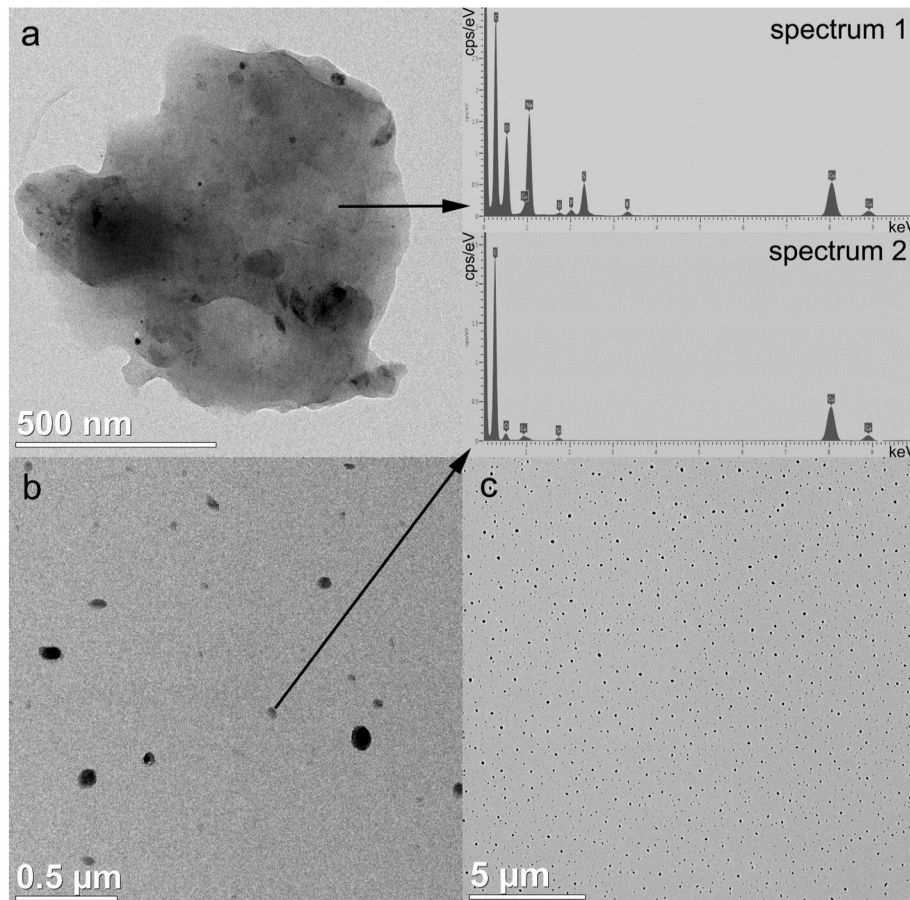
Fig. 5. TEM bright field images of particles on PP$_{OP}$ injection molding sample taken during day 2 at 1:36 a) mixed particle and accordingly marked energy-dispersive spectroscopy chemical composition (spectrum 1); b) carbon based (spectrum 2) and other, S-containing particles (spectrum assimilates 1); c) overview image of carbon based and S-containing particles.

the presence of micron-sized particles, which can impact on the diffusion stage. Even though the DiSCmini has a pre-seperator with a 0.7 μm D_{50} value, some larger particles can still penetrate it, which may cause measurement problems. For example, a spherical 3 μm particle will have the same diffusion stage penetration as a 40 nm particle, but due to the $D_p^{1.1}$ dependency, it will carry a roughly 100 times higher charge. It will therefore be interpreted as 100 small sized particles (Fierz et al., 2011). Furthermore, as the D_{50} value of the pre-separator concerns aerodynamic diameters, larger mobility size agglomerates with particle density < 1 g cm^{-3} may still penetrate to the instrument at high probability. The TEM images form samples taken in the WCCo production plant showed irregular shaped agglomerated particles of different sizes, which likely have a lower density than their compact material equivalent. The samples from the injection molding showed indication for large, droplet like particles. The collected particle might have been more homogenous and compact than the agglomerated particles collected during sieving and milling. The LDSA concentrations varied from 10.0 to 18.7 μm^2 cm^{-3}. The concentrations were below one GSD from urban background geometric mean concentrations of 20 μm^2 cm^{-3}.

4.1. Knowledge gaps in first order risk assessment for inhalation exposure based upon pulmonary inflammation

Table 1 show that there are major knowledge gaps in all steps of the risk assessment: the exposure, dose, and dose-response assessment. Regarding exposure, workplace air PM characterization and conceptual information including working practices and work load are critical when estimating exposure and dose of process particles. With respect to hazard assessment, toxicological comparability of particles found at the work place and the GBPs and transition metal oxide particles used in previous dose-response assessment should be verified preferably with dose-response studies using the particles collected from the workplace air. Biodurability of particles at the workplaces should be verified. Kühnel et al. (2012) showed that dissolution of tungsten and cobalt from WCCo particles in Roswell Park Memorial Institute Medium with and without 5% fetal bovine serum was 15% W and 76% Co after one week.

The majority of the uncertainties are related to extrapolation from dose-response data based on dry powder BET measurements of particles following intratracheal instillations to the human equivalent LDSA dose-response (Table 1). The relation between dry powder BET surface area and LDSA should be studied for different materials for dose conversion. This requires well-controlled inhalation studies where the airborne particles BET surface area concentrations, LDSA concentrations, and size resolved particle concentrations are measured. After inhalation of high particle concentrations the deposited particles may agglomerate in the lung which effect on the BET surface area (Mercer et al., 2013). The calculated deposited doses from measured concentrations should be compared with actual deposited dose measured from lung tissue to understand range of the uncertainty. The dose-responses following inhalation exposures should be compared with the dose-responses determined in instillation studies to understand correlation between inhalation uptake and instilled dose.

5. Conclusions

In this study, a workers risk to suffer acute pulmonary inflammation was estimated by measuring alveolar lung deposited surface area (LDSA) concentrations which were used to calculate process specific
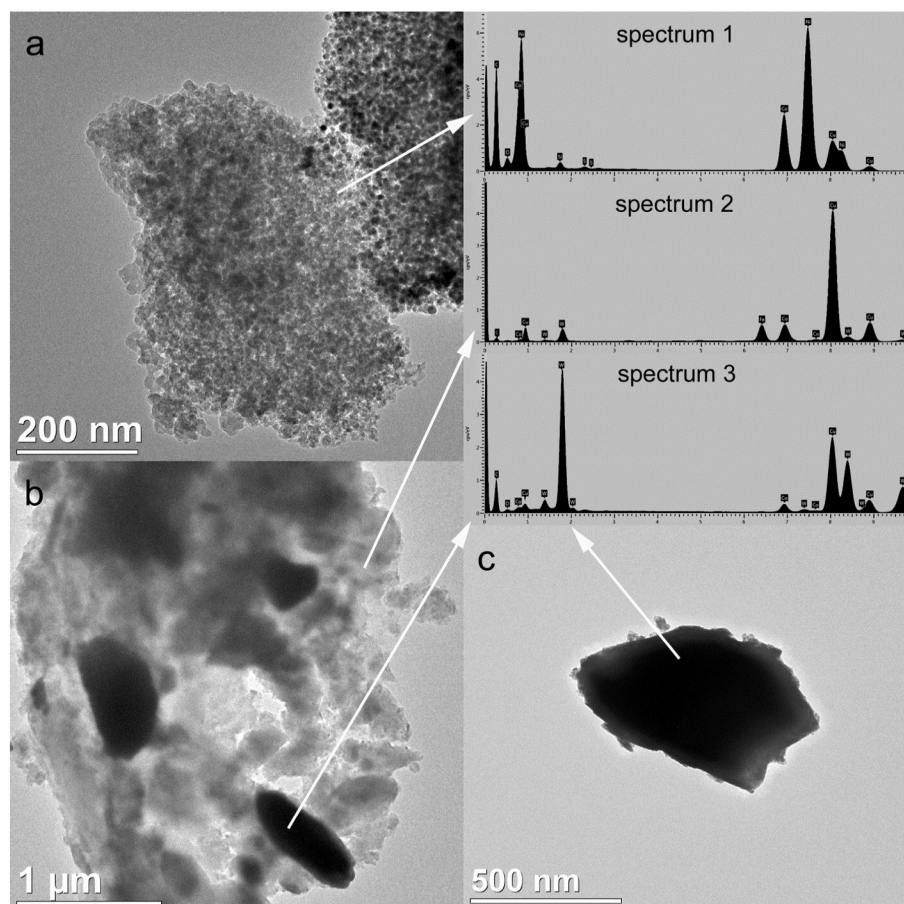
Fig. 6. TEM bright field images of particles on sieving and milling sample taken at 1:18 a) NiP aggregate; b) Tungsten-carbide-cobalt (WCCo) internally mixed FeCu; c) Tungsten-carbide-cobalt (WCCo) particle, and their accordingly marked energy-dispersive spectroscopy chemical composition.

8-h doses. The acute pulmonary inflammation risk was estimated by comparing 8-h doses with the no observed effect level divided with a 100 factor ($NOEL_{1/100}$). The injection molding of polypropylene (PP) car bumpers did not notably increase process site concentrations from the far field levels which ranged from 23 to 39.8 $\mu m^2 \, cm^{-3}$ but during PP material change was measured an increase of on average 10 $\mu m^2 \, cm^{-3}$. The 8-h PP particle doses were at maximum $1.4 \times 10^{-3} \, cm^2 \, g^{-1}$ which was lower by a factor 100 compared to the $NOEL_{1/100}$ of 0.11 $cm^2 \, g^{-1}$ assigned for granular biodurable particles. In the WCCo fine powder production plant, the LDSA concentrations were below 18.7 $\mu m^2 \, cm^{-3}$ which corresponds to the 8-h dose of $2.7 \times 10^{-3} \, cm^2 \, g^{-1}$ being 3 times below the $NOEL_{1/100}$ of $9 \times 10^{-3} \, cm^2 \, g^{-1}$ for transition metal oxide particles. In general, the LDSA concentrations were low compared to average geometric mean urban background levels of 44.2 $\mu m^2 \, cm^{-3}$ in European cities.

Acknowledgement

References

Arts, J.H., Hadi, M., Irfan, M.A., Keene, A.M., et al., 2015. A decision-making framework for the grouping and testing of nanomaterials (DF4nanoGrouping). Regul. Toxicol. Pharmacol. 71, S1–S27.

Arts, J.H., Hadi, M., Keene, A.M., Kreiling, R., Lyon, D., Maier, M., et al., 2014. A critical appraisal of existing concepts for the grouping of nanomaterials. Regul. Toxicol. Pharmacol. 70, 492–506.

Arts, J.H., Irfan, M.A., Keene, A.M., Kreiling, R., Lyon, D., Maier, M., et al., 2016. Case studies putting the decision-making framework for the grouping and testing of nanomaterials (DF4nanoGrouping) into practice. Regul. Toxicol. Pharmacol. 76, 234–261.

Asbach, C., Fissan, H., Stahlmecke, B., Kuhlbusch, T.A.J., Pui, D.Y.H., 2009. Conceptual limitations and extensions of lung-deposited nanoparticle surface area monitor (NSAM). J. Nanopart. Res. 11, 101–109.

Asbach, C., Kaminski, H., von Barany, D., Kuhlbusch, T.A., Monz, C., Dziurowitz, N., et al., 2012. Comparability of portable nanoparticle exposure monitors. Ann. Occup. Hyg. 56, 606–621.

Baisch, B.L., Corson, N.M., Wade-Mercer, P., Gelein, R., Kennell, A.J., Oberdörster, G., et al., 2014. Equivalent titanium dioxide nanoparticle deposition by intratracheal instillation and whole body inhalation - the effect of dose rate on acute respiratory tract inflammation. Part. Fibre Toxicol. 11, 5.

Bau, S., Zimmermann, B., Payet, R., Witschger, O., 2014. A laboratory study of the performance of the handheld diffusion size classifier (DiSCmini) for various aerosols in the 15–400 nm range. Environ. Sci. Process Impacts. 17, 261–269.

Bekker, C., Kuijpers, E., Brouwer, D.H., Vermeulen, R., Fransman, W., 2015. Occupational exposure to nano-objects and their agglomerates and aggregates across various life cycle stages; a broad-scale exposure study. Ann. Occup. Hyg. 59, 681–704.

Boonruksa, P., Bello, D., Zhang, J., Isaacs, J.A., Mead, J.L., Woskie, S.R., 2016. Characterization of potential exposures to nanoparticles and fibers during manufacturing and recycling of carbon nanotube reinforced polypropylene composites. Ann. Occup. Hyg. 60, 40–55.

Borm, P.J.A., Kelly, F., Künzli, N., Schins, R.P.F., Donaldson, K., 2007. Oxidant generation by particulate matter from biologically effective dose to a promising, novel metric. Occup. Environ. Med. 64, 73–74.

Braakhuis, H.M., Cassee, F.R., Fokkens, P.H.B., de la Fonteyne, L.J., Oomen, A.G., Krystek, P., et al., 2016. Identification of the appropriate dose metric for pulmonary inflammation of silver nanoparticles in an inhalation toxicity study. Nanotoxicology 10, 63–73.

Brown, J.S., Wilson, W.E., Grant, L.D., 2005. Dosimetric comparisons of particle deposition and retention in rats and humans. Inhal. Toxicol. 17, 355–386.

Buonanno, G., Marini, S., Morawska, L., Fuoco, F.C., 2012. Individual dose and exposure of Italian children to ultrafine particles. Sci. Total Environ. 438, 271–277.

Buonanno, G., Morawska, L., Stabile, L., 2011. Exposure to welding particles in automotive plants. J. Aerosol Sci. 42, 295–304.

Buonanno, G., Morawska, L., Stabile, L., Viola, A., 2010. Exposure to particle number, surface are and PM concentrations in pizzerias. Atmos. Environ. 44, 3963–3969.

Cherrie, J.W., Brosseau, L.M., Hay, A., Donaldson, K., 2013. Low-toxicity dusts: current exposure guidelines are not sufficiently protective. Ann. Occup. Hyg. 57, 685–691.

Dekkers, S., Oomen, A.G., Bleeker, E.A.J., Vandebriel, R.J., Micheletti, C., Cabellos, J., et al., 2016. Towards a nanospecific approach for risk assessment. Regul. Toxicol. Pharmacol. 80, 46–59.

ECHA, 2009. TNsG on Annex I Inclusion. Revision of Chapter 4.1: Quantitative Human Health Risk Characterisation. (Available online: https://echa.europa.eu/documents/10162/16960215/revision_tnsg_annex_i_inclusion_chapter_4.1_2009_en.pdf (accessed on 19 July 2016)).

ECHA, 2016. Guidance on Information Requirements and Chemical Safety Assessment. Chapter R.15: Consumer Exposure Assessment. (Available online: https://echa.europa.eu/documents/10162/13632/information_requirements_r15_en.pdf (accessed on 19 July 2016)).

Eeftens, M., Phuleria, H.C., Meier, R., Aguilera, I., Corradi, E., Davey, M., et al., 2015. Spatial and temporal variability of ultrafine particles, NO_2, $PM_{2.5}$, $PM_{2.5}$ absorbance, PM10 and PM_{coarse} in Swiss study areas. Atmos. Environ. 111, 60–70.

Fierz, M., Houle, C., Steigmeier, P., Burtscher, H., 2011. Design, calibration, and field performance of a miniature diffusion size classifier. Aerosol Sci. Technol. 45, 1–10.

Freijer, J.I., Cassee, F.R., Van Bree, L., 1997. Modelling of Particulate Matter Deposition in the Human Airways (RIVM report 624029001).

Gebel, T., Foth, H., Damm, G., Freyberger, A., Kramer, P.J., Lilienblum, W., et al., 2014. Manufactured nanomaterials: categorization and approaches to hazard assessment. Arch. Toxicol. 88, 2191–2211.

Gebel, T., 2012. Small difference in carcinogenic potency between GBP nanomaterials and GBP micromaterials. Arch. Toxicol. 86, 995–1007.

Geiss, O., Bianchi, I., Barrero-Moreno, J., 2016. Lung-deposited surface area concentration measurements in selected occupational and non-occupational environments. J. Aerosol Sci. 96, 24–37.

Godwin, H., Nameth, C., Avery, D., Bergeson, L.L., Bernard, D., Beryt, E., et al., 2015. Nanomaterial categorization for assessing risk potential to facilitate regulatory decision-making. ACS Nano 9, 3409–3417.

Gomes, J.F., Bordado, J.C., Albuquerque, P.C., 2012. On the assessment of exposure to airborne ultrafine particles in urban environments. J. Toxicol. Environ. Health 75, 1316–1329.

Grommes, J., Soehnlein, O., 2011. Contribution of neutrophils to acute lung injury. Mol. Med. 17, 293–307.

Horie, M., Yoshiura, Y., Izumi, H., Oyabu, T., Tomonaga, T., Okada, T., et al., 2016. Comparison of the pulmonary oxidative stress caused by intratracheal instillation and inhalation of NiO nanoparticles when equivalent amounts of NiO are retained in the lung. Antioxidants 18, 5 (Basel).

Hussain, M., Madl, P., Khan, A., 2011. Lung deposition predictions of airborne particles and the emergence of contemporary diseases part-I. The Health 2, 51–59.

Hämeri, K., Lähde, T., Hussein, T., Koivisto, J., Savolainen, K., 2009. Facing the key workplace challenge: assessing and preventing exposure to nanoparticles at source. Inhal. Toxicol. 21, 17–24.

Janssen, L.L., Nelson, T.J., Cuta, K.T., 2007. Workplace protection factors for an N95 filtering facepiece respirator. J. Occup. Environ. Hyg. 4, 698–707.

Jarabek, A.M., Asgharian, B., Miller, F.J., 2005. Dosimetric adjustments for interspecies extrapolation of inhaled poorly soluble particles (PSP). Inhal. Toxicol. 17, 317–334.

Ku, B.K., Kulkarni, P., 2012. Comparison of diffusion charging and mobility-based methods for measurement of aerosol agglomerate surface area. J. Aerosol Sci. 47, 100–110.

Ku, B.K., Maynard, A.D., 2005. Comparing aerosol surface-area measurements of monodisperse ultrafine silver agglomerates by mobility analysis, transmission electron microscopy and diffusion charging. J. Aerosol Sci. 36, 1108–1124.

Kuempel, E.D., Attfield, M.D., Stayner, L.T., Castranova, V., 2014. Human and animal evidence supports lower occupational exposure limits for poorly-soluble respirable particles. Ann. Occup. Hyg. 58, 1–4.

Kühnel, D., Scheffler, K., Wellner, P., Meißner, T., Potthoff, A., Busch, W., Springer, A., Schirmer, K., 2012. Comparative evaluation of particle properties, formation of reactive oxygen species and genotoxic potential of tungsten carbide based nanoparticles in vitro. J. Hazard. Mater. 15 (227–228), 418–426.

LeBouf, R.F., Ku, B.K., Chen, B.T., Frazer, D.G., Cumpston, J.L., Stefaniak, A.B., 2011. Measuring surface area of airborne titanium dioxide powder agglomerates: relationships between gas adsorption, diffusion and mobility-based methods. J. Nanopart. Res. 13, 7029–7039.

Lison, D., Vietti, G., van den Brule, S., 2014. Paracelsus in nanotoxicology. Part. Fibre Toxicol. 11, 35.

Maintz, M.F., 2015. Applications of synthetic polymers in clinical medicine. Biosurface and Biotribology 1, 161–176.

Maynard, A.D., Kuempel, E.D., 2005. Airborne nanostructured particles and occupational health. J. Nanopart. Res. 7, 587–614.

Mercer, R.R., Scabilloni, J.F., Hubbs, A.F., Battelli, L.A., McKinney, W., Friend, S., Wolfarth, M.G., Andrew, M., Castranova, V., Porter, D.W., 2013. Distribution and fibrotic response following inhalation exposure to multi-walled carbon nanotubes. Part. Fibre Toxicol. 10, 33.

Molina, D.K., DiMaio, V.J., 2012. Normal organ weights in men: part II-the brain, lungs, liver, spleen, and kidneys. Am. J. Forensic Med. Pathol. 33, 68–372.

Moreno-Horn, M., Gebel, T., 2014. Granular biodurable nanomaterials: no convincing evidence for systemic toxicity. Crit. Rev. Toxicol. 44, 849–875.

Morimoto, Y., Izumi, H., Yoshiura, Y., Fujishima, K., Yatera, K., Yamamoto, K., 2016. Usefulness of intratracheal instillation studies for estimating nanoparticle-induced pulmonary toxicity. Int. J. Mol. Sci. 17, 165.

Nieboer, E., Thomassen, Y., Chashchin, V., Odland, J.O., 2005. Occupational exposure assessment of metals. J. Environ. Monit. 7, 411–415.

Ntziachristos, L., Polidori, A., Phuleria, H., Geller, M.D., Sioutas, C., 2007. Application of a diffusion charger for the measurement of particle surface concentration in different environments. Aerosol Sci. Technol. 41, 571–580.

Oberdörster, G., 2000. Toxicology of ultrafine particles: in vivo studies. Philos. Trans. R. Soc. Lond. A Math. Phys. Eng. Sci. 358, 2719–2740.

Oberdörster, G., Oberdörster, E., Oberdörster, J., 2005. Nanotoxicology: an emerging discipline evolving from studies of ultrafine particles. Environ. Health Perspect. 113, 823–839.

OECD, 2015. Harmonized tiered approach to measure and assess the potential exposure to airborne emissions of engineered nano-objects and their agglomerates and aggregates at workplaces. Paris, France: Series on the Safety of Manufactured Nanomaterials No. 55. Organisation for Economic Co-operation and Development (ENV/JM/MONO (2015) 19).

Oller, A.R., Oberdörster, G., 2010. Incorporation of particle size differences between animal studies and human workplace aerosols for deriving exposure limit values. Regul. Toxicol. Pharmacol. 57, 181–194.

Piccinno, F., Gottschalk, F., Seeger, S., Nowack, B., 2012. Industrial production quantities and uses of ten engineered nanomaterials in Europe and the world. J. Nanopart. Res. 14, 1109.

Pietroiusti, A., Magrini, A., 2014. Engineered nanoparticles at the workplace: current knowledge about workers' risk. Occup. Med. (Lond.) 64, 319–330.

R'mili, B., Le Bihan, O.L.C., Dutouquet, C., Aguerre-Charriol, O., Frejafon, E., 2013. Particle sampling by TEM grid filtration. Aerosol Sci. Technol. 47, 767–775.

Reche, C., Querol, X., Alastuey, A., Viana, M., Pey, J., Moreno, T., et al., 2011. New considerations for PM, black carbon and particle number concentration for air quality monitoring across different European cities. Atmos. Chem. Phys. 11, 6207–6227.

Schmid, O., Stoeger, T., 2016. Surface area is the biologically most effective dose metric for acute nanoparticle toxicity in the lung. J. Aerosol Sci. 99, 133–143.

Simkó, M., Nosske, D., Kreyling, W.G., 2014. Metrics, dose, and dose concept: the need for a proper dose concept in the risk assessment of nanoparticles. Int. J. Environ. Res. Public Health 11, 4026–4048.

Sotiriou, G.A., Singh, D., Zhang, F., Chalbot, M.-C.G., Spielman-Sun, E., Hoering, L., et al., 2016. Thermal decomposition of nano-enabled thermoplastics - possible environmental health and safety implications. J. Hazard. Mater. 305, 87–95.

Spinazzè, A., Cattaneo, A., Scocca, D.R., Bonzini, M., Cavallo, D.M., 2015. Multi-metric measurement of personal exposure to ultrafine particles in selected urban microenvironments. Atmos. Environ. 110, 8–17.

Stoeger, T., Takenaka, S., Frankenberger, B., Ritter, B., Karg, E., Maier, K., et al., 2009. Deducing in vivo toxicity of combustion-derived nanoparticles from a cell-free oxidative potency assay and metabolic activation of organic compounds. Environ. Health Perspect. 117, 54–60.

Stoeger, T., Schmid, O., Takenaka, S., Schulz, H., 2007. Inflammatory response to TiO2 and carbonaceous particles scales best with BET surface area. Environ. Health Perspect. 115, A290–A291.

Todea, A.M., Beckmann, S., Kaminski, H., Asbach, C., 2015. Accuracy of electrical aerosol sensors measuring lung deposited surface area concentrations. J. Aerosol Sci. 89, 96–109.

Vance, M.E., Kuiken, T., Vejerano, E.P., McGinnis, S.P., Hochella Jr., M.F., Rejeski, D., et al., 2015. Nanotechnology in the real world: redeveloping the nanomaterial consumer products inventory. Beilstein J. Nanotechnol. 6, 1769–1780.

Vu, T.V., Delgado-Saborit, J.M., Harrison, R.M., 2015. A review of hygroscopic growth factors of submicron aerosols from different sources and its implication for calculation of lung deposition efficiency of ambient aerosols. Air Qual. Atmos. Health 8, 429–440.

Waters, K.M., Masiello, L.M., Zangar, R.C., Tarasevich, B.J., Karin, N.J., Quesenberry, R.D., et al., 2009. Macrophage responses to silica nanoparticles are highly conserved across particle sizes. Toxicol. Sci. 107, 553–569.

Wittmaack, K., 2007. In search of the most relevant parameter for quantifying lung inflammatory response to nanoparticle exposure: particle number, surface area, or what? Environ. Health Perspect. 115, 187–194.